

DUCTILITY ESTIMATION OF FIXED-HEAD Laterally LOADED PILE: AN ANALYTICAL MODEL

M. Teguh^{1*}, F. Saleh²

¹ *Department of Civil Engineering, Islamic University of Indonesia, Indonesia*

² *Department of Civil Engineering, Muhammadiyah University of Yogyakarta, Indonesia*

ABSTRACT

During seismic event, a series of large curvature demand and plastic hinges due to restraint at the anchorage headed reinforcement in reinforced concrete (RC) piles may occur along slender piles and at a fixed-head pile foundation system. Limiting the curvature ductility demand in the potential plastic hinge region of the pile and increasing the displacement ductility demand at the pile head connection produce rigorousness of local damage at the pile foundation system. The strength and stiffness of the soil-pile system as well as the equivalent plastic hinge length of the pile have contributed to the curvature ductility demand. A kinematic model in conjunction with the displacement ductility factor to the local curvature ductility demand based on the limit state analysis of pile-to-pile cap connections with a particular attention on the fixed-head case was theoretically performed. For simplicity purposes, a limit state analysis of laterally loaded piles is analytically studied to propose a numerical procedure outlined in a flow chart. The flow chart for assessing ductility demand of fixed-head pile-to-pile cap connections has identified its application to the pile-to-pile cap connection embedded in two different soil conditions. For practical exercises, a detail computational procedure was provided in a companion paper.

Keywords: Curvature demand; Ductility demand; Fixed-head; Pile-to-pile cap connection; Plastic hinge

1. INTRODUCTION

The seismic response of pile foundation systems due to strong ground motion is mainly affected by inertial interaction between superstructure and pile foundation, kinematic interaction between foundation soils and piles, and the nonlinear stress-strain behaviour of soils and the soil-pile interface (Holmes, 2000). Given this condition, the seismic response of fixed-head laterally loaded pile foundation is a very complicated analysis. According to Gazetas et al. (1992), Matlock and Reese (1960), the soil surrounding piles under such extreme conditions may experience serious problems resulting plastic hinges at the pile-to-pile cap connection and buckling along the pile. An evidence showed that the main pile supported structures located on soft soils in the earthquake prone area produced major demands on the pile foundation systems. Significant effect between longer period of soft soil zones, which may potentially amplify ground motions and large structures can exacerbate the pile foundation problem (Meymand 1998).

* Corresponding author's email: m.teguh@uii.ac.id

Simplified and non-standardized analysis methods are commonly utilized to evaluate pile capacity during a severe earthquake event. It has been observed that pile performance during earthquakes produces two principal facts emerge; namely, that pile foundations influence the ground motions that the superstructure experiences; and the pile suffers extreme damage and failure under seismic loading. In fact, well-documented seismic soil-pile response based on case histories that record dynamic response is still limited. The partial database of measured pile performance during earthquakes produces inadequate data for calibrating and validating the available analytical methods to develop the seismic soil-pile-superstructure interaction problems. In general, seismic soil-pile-superstructure interaction (SSPSI) is classified into the subsequent interaction modes: kinematic, inertial, radiation, and soil-pile. As an example, Gazetas et al. (1992) developed a global schematic of the principal characteristics of SSPSI for a single pile, as shown in Figure 1.

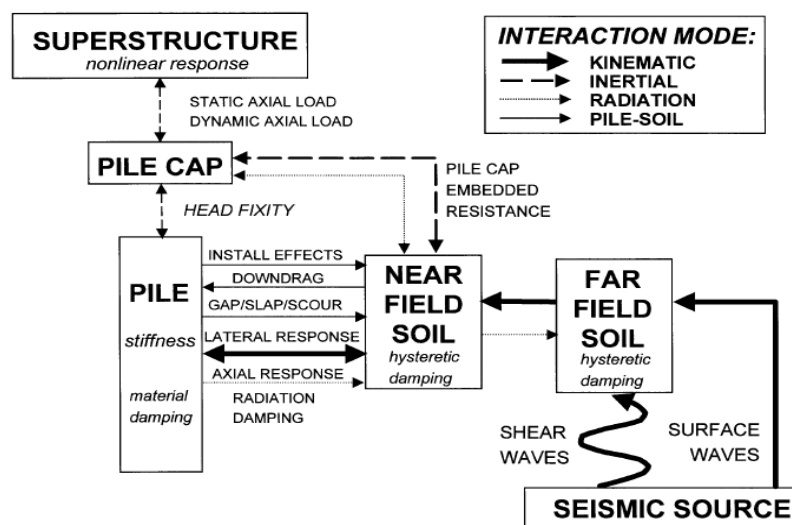


Figure 1. Schematic of modes of single pile seismic response (Gazetas et al. 1992)

The system components comprise the superstructure, pile cap, pile, soil and seismic energy source. The soil is idealized into near field and far field domains. The modes of system interaction incorporate kinematic, inertial, and physical interaction, and radiation damping. Since the SSPSI is a major area of geotechnical engineering that directly correlates to the structural engineering field, soil-pile interaction was adopted and integrated in the current analytical study of pile-to-pile cap connections. For this reason, the soil-pile interaction mode has been taken into account in this study with regard to model ductility assessment of the pile-to-pile cap connections, whilst other interactions are excluded. The following sections present the theoretical soil-pile interaction in conjunction with the ductility assessment of the fixed-head pile connections. An application of simplified lateral load analyses of a fixed-head pile was briefly described in a companion paper (Teguh, 2009).

The main objective of this paper, therefore, is to analytically model the ductility assessment of the pile-to-pile cap connections utilizing a limit states analysis of laterally loaded piles with a particular attention on a fixed-head case. This study provides the theoretical background and a simplified model of the soil-pile interaction for the development of proposed pile-to-pile cap connections.

2. LIMIT STATE ANALYSIS

2.1. Fixed-head Concrete Pile Foundation

Deep pile-foundation systems supporting heavy superstructures are commonly used concrete piles with regard to restrain rotation at the pile head. It should be noted that anchoring the pile reinforcement into the pile cap is essential to sufficiently produce yield strength in the headed reinforcement. Establishment of a plastic hinge in the single pile shaft is a mechanism of ductile performance that may be achieved. At early stage of deformation in the fixed-head pile, a plastic hinge is formed at the interface between pile head and pile cap, whilst the flexural capacity can be obtained through the formation of a secondary, i.e. subgrade hinge. On the other hand, the inelastic deformation of a free-head pile forms at the point of maximum moment located in the shaft below grade level. The effect of fixity at the pile-to-pile cap connection subjected to lateral seismic loads induces a large curvature demand at the pile head, with potential for severe damage or failure of the pile. In the analysis of piles, different techniques of the sophisticated finite element method proposed by Yang and Jeremic (2002) are possibly adopted by utilizing a simpler approach and characterizing the response of the pile for a selected number of limit states. According to Song et al. (2005), a laterally loaded fixed-head pile can be expressed by a sequential yielding of the pile that occurs until a plastic mechanism is fully achieved (Figure 2).

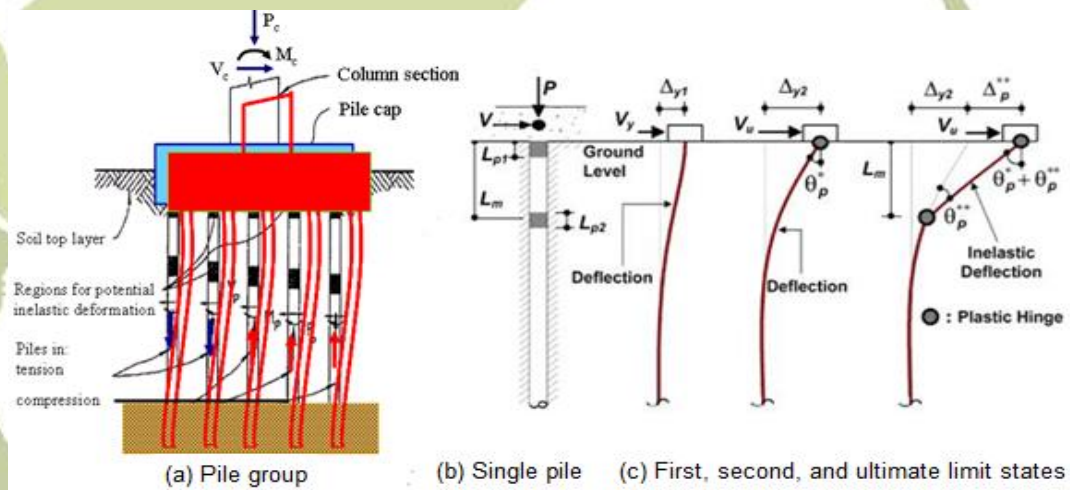


Figure 2. Deformed pile and limit states distribution of a laterally loaded fixed-head pile

A deformed pile group is shown in Figure 2a, while a series of lateral displacement beyond the first, second, and ultimate limit states on a single pile are briefly illustrated in Figure 2b-c. This involves a concentrated plastic rotation of the hinge, which is accompanied by a redistribution of internal forces in the pile. The redistribution increases the flexural moment in the non-yielding portion of the pile until the formation of the second plastic hinge is developed. The first yield limit state of the pile is characterized by a maximum bending moment, M_u , at the pile-to-pile cap connection reaching the flexural strength of the pile. A plastic hinge is assumed to form with the center of rotation occurring at ground level. The bending moment distribution below the plastic hinge diminishes with depth and reverses in direction, leading to a local

maximum bending moment, M_{max} , at a depth L_m' . Displacement beyond the first yield limit state involves a concentrated plastic rotation of the hinge, which is accompanied by a redistribution of internal forces in the pile. The redistribution increases the bending moment in the non-yielding portion of the pile until the formation of the second plastic hinge. The second yield limit state where the second plastic hinge forms at depth, L_m , is smaller than the initial depth at the maximum moment, L_m' . As the location of the maximum bending moment migrates toward the ground surface, the curvature ductility demand then increases due to a smaller lever arm. Continued lateral displacement altering the second plastic hinge formation is facilitated by inelastic rotations at both plastic hinges until the pile reaches the ultimate limit state.

In this study, the ultimate limit state is assumed to be associated with flexural failure as a consequence of long pile, and as dictated by an ultimate curvature in either the first or the second plastic hinge. The identification of these limit states allows a simple mechanistic model to be developed so that the lateral stiffness and strength of the soil-pile system, as well as the curvature ductility demand, can be estimated. Seismic performance of fixed-head piles depends on the level of inelastic deformation imposed on the pile. Inelastic deformation is generally characterized in terms of curvature demand with regard to the stiffness and strength of the soil-pile system, and the plastic hinge length of the pile. A kinematic model in conjunction with the displacement ductility factor and curvature ductility factor proposed by Song et al. (2005) was mainly adopted and is discussed in the following sections for proposing a flow chart to simplify a computation. In the limit state derivation, it is considered that the pile is fully embedded in cohesive and cohesionless soils (Reese and Van Impe, 2001).

2.2. Lateral stiffness of different soil condition

2.2.1. Cohesive soils

According to Poulos and Davis (1980), utilizing the Winkler foundation concept, the soil can be replaced with a series of springs, which provides a soil reaction that is proportional to the lateral deflection. The stiffness of the soil-spring is assumed to be independent of the depth, resulting in a constant horizontal subgrade reaction, k_h . For a fixed-head pile with an imposed lateral displacement, Δ , at the ground level, the lateral stiffness of soil-pile system, K_p , due to the lateral force, V , is written as $K_p = 1.414(E_p I_p / R_c^3)$, where $E_p I_p$ is the effective flexural rigidity of the pile and the characteristic length of the pile, R_c , is defined as $R_c \equiv \sqrt[4]{E_p I_p / k_h}$. The lateral deflection, Δ_{y1} , at the ground level of the 1st yield limit state is determined by equating the flexural moment at the pile-to-pile cap connection to the ultimate moment capacity, M_u , of the pile, supposing an elasto-plastic moment curvature response is expressed in Eq. (1) as follows:

$$\Delta_{y1} = \frac{M_u R_c^2}{E_p I_p} \quad (1)$$

The lateral force, V_y , at the first plastic hinge written in Eq. (2) is determined by multiplying the lateral stiffness, K_p , with the first yield displacement, Δ_{y1} . Whilst the

reduced lateral stiffness, K_{rp} , and the corresponding plastic rotation, θ , at the ground level after the first yield limit state are expressed in Eq. (3) as follows:

$$V_y = 1.414 \frac{M_u}{R_c} \quad (2)$$

$$K_{rp} = \frac{E_p I_p}{1.414 R_c^3} \quad \text{and} \quad \theta = \frac{\Delta - \Delta_{y1}}{1.414 R_c} \quad \text{for } V > V_y \text{ and } \Delta > \Delta_{y1} \quad (3)$$

An estimation of the modulus of horizontal subgrade reaction, k_h , for cohesive soil has been proposed by Davisson and Salley (1970) and Poulos and David (1980) as the simple expression, $k_h = 67 s_u$, where s_u is the undrained shear strength of the cohesive soil, which is obtained from field tests or site classifications in current building codes such as NEHRP (2001) or ATC-40 (1996).

2.2.2. Cohesionless soils

Studies on the magnitude and distribution of the ultimate soil pressure on piles in cohesionless soils had been reported in the past, and an ultimate lateral pressure distribution for design was proposed by Broms (1964). The lateral pressure, p_u , on the pile is then taken to be equal to 3 times the Rankine passive pressure of the soil, $p_u(x) = 3 \sigma'_v(x) \bar{K}_p$. The vertical effective overburden stress, $\sigma'_v(x)$, is taken as the effective unit weight, γ' , multiplied by the depth x , and the term \bar{K}_p is the coefficient of passive soil pressure and is given by $\bar{K}_p = (1 + \sin \bar{\phi}) / (1 - \sin \bar{\phi})$. It is noted that the ultimate pressure distribution, which varies linearly with depth. The depth at which the second plastic hinge forms, L_m , and the ultimate lateral strength of the soil-pile system, V_u , can be determined using the ultimate soil pressure distribution, $p_u(x)$. The normalized depth to the second plastic hinge, defined as $L_m^* \equiv L_m / D$, the normalized ultimate lateral strength, defined as $V_u^* \equiv V_u / (\bar{K}_p \gamma' D^3)$, and the normalized flexural strength, defined as $M_u^* \equiv M_u / (\bar{K}_p \gamma' D^4)$, for piles in cohesionless soils, are expressed in Eq. 4 and Eq. 5 as follows:

$$L_m^* = 1.26 \left(\sqrt[3]{\frac{M_u}{\bar{K}_p \gamma' D^4}} \right) \quad (4)$$

$$V_u^* = 1.5 \left(\frac{L_m}{D} \right)^2 \quad (5)$$

3. KINEMATIK RELATION

The severity of local damage is determined by limiting the curvature ductility demand in the potential plastic hinge region. The curvature ductility demand, which is different for the two plastic hinges, depends on the displacement ductility imposed on the pile. Figure 3 can be used to estimate the local inelastic deformation in the critical region, where the lateral response of a fixed-head pile is estimated by a tri-linear force-displacement response, with an initial stiffness, K_p , followed by a reduced stiffness, K_{rp} .

The lateral displacements Δ_{y1} and Δ_{y2} are used to define the first and second yield limit states. The lateral displacement beyond, Δ_{y2} , is characterized by a constant lateral force signifying a fully plastic response. The ultimate limit state, defined as the ultimate lateral displacement, Δ_u , depends on the ductility capacity of the plastic hinges. The lateral force-displacement response of the fixed-head pile can be idealized by a bilinear elastoplastic response with the equivalent-elastoplastic yield displacement, Δ_y . The displacement ductility factor, μ_Δ , is then defined as ratio of the ultimate lateral displacement, Δ_u , and the equivalent elastoplastic yield displacement, Δ_y , where Δ_p^* is the increased plastic displacement from the stage of second plastic hinge formation to the ultimate limit state.

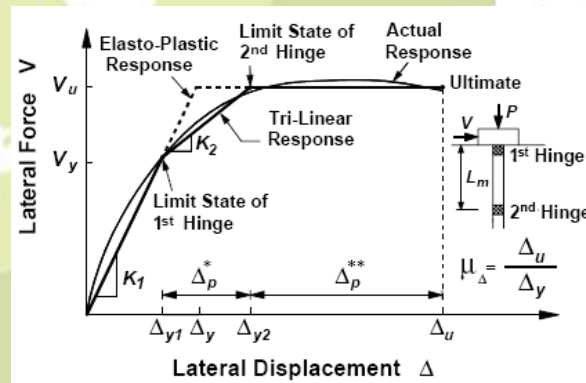


Figure 3. Determination of the displacement ductility factor for fixed-head piles.

Eq. (6) presents the equivalent-elastoplastic yield displacement, Δ_y , which is formulated based on a ratio of the ultimate lateral strength, V_u , and the initial stiffness, K_p , of the bilinear curve:

$$\Delta_y = \frac{V_u}{K_p} \text{ and } \Delta_{y1} = \frac{V_y}{K_p} \tag{6}$$

where V_y is the lateral force required to produce the first plastic hinge, and similarly the lateral displacement at the second yield limit state, Δ_{y2} can be defined from the idealized trilinear response as denoted in Eq. (7).

$$\Delta_{y2} = \frac{V_y}{K_p} + \frac{V_u - V_y}{K_{rp}} \tag{7}$$

It is clearly shown in Figure 3, from Δ_{y2} to Δ_u produces a rotation of θ_p^{**} in both plastic hinges. The θ_p^{**} , is defined as a ratio of the Δ_p^{**} , and the depth to the second plastic hinge, L_m , or $\theta_p^{**} = \Delta_p^{**} / L_m$, where $L_m = L_m^* D$. To estimate the curvature ductility, the plastic rotation is uniformly distributed over the plastic hinge. At the first plastic hinge, the θ_p^{**} is written as $\theta_p^{**} = (\phi_{u1} - \phi_i) L_{p1}$ for $\phi_{u1} \geq \phi_i \geq \phi_y$, where ϕ_i is the curvature in the first plastic hinge at the lateral displacement, Δ_{y2} , ϕ_{u1} is the ultimate curvature in the first plastic hinge, and L_{p1} is the equivalent plastic hinge length for the first hinge condition. When the first plastic hinge length to $\lambda_{p1} \equiv L_{p1} / D$ is normalized and combines with

the θ_p^{**} produces the plastic displacement, $\Delta_p^{**} = (\phi_{u1} - \phi_i) \lambda_{p1} L_m^* D^2$. Having a relation of the Δ_y , Δ_{y2} and Δ_p^{**} provides a relation between the displacement ductility factor and the curvature demand in the first plastic hinge. Determining the coefficients $\alpha \equiv V_y / V_u = \Delta_{y1} / \Delta_u$ and $\beta \equiv \Delta_y / (\phi_y L_m^2)$, the displacement ductility factor, μ_Δ , is a function of the curvature ductility factor, $\mu_{\phi1}$, in the first plastic hinge as denoted in Eq. (8), where $\mu_{\phi1} \equiv \phi_{u1} / \phi_y$ and $\mu_{\phi i} \equiv \phi_{ui} / \phi_y$ is the curvature ductility demand in the first plastic hinge at Δ_{y2} .

$$\mu_\Delta = \alpha + \frac{K_p}{K_{rp}} (1 - \alpha) + \frac{\lambda_{p1}}{\beta L_m^*} (\mu_{\phi1} - \mu_{\phi i}) \quad (8)$$

The kinematic relation in Eq. (8) requires the determination of the curvature ductility, $\mu_{\phi i}$, which involves the plastic rotation of the first plastic hinge at the lateral displacement, Δ_{y2} . The plastic displacement, $\Delta_p^* = \Delta_{y2} - \Delta_{y1}$ is associated with a plastic rotation, θ_p^* , in the first plastic hinge. Supposing a uniform distribution of plastic rotation in the plastic hinge, the curvature ductility factor, $\mu_{\phi i} = 1 + \theta_p^* / (\phi_y L_{p1})$, is a function of the plastic rotation, θ_p^* .

The plastic rotation, θ_p^* , is then determined by the expression of pile head rotation, $\theta = (\Delta - \Delta_{y1}) / 1.414 R_c$ for cohesive soils and $\theta = 2(\Delta - \Delta_{y1}) / 3 R_n$ for cohesionless soils. Replacing the numerator $(\Delta - \Delta_i)$ with Δ_p^* in both equations, the plastic rotation, θ_p^* , can be easily written as $\theta_p^* = \Delta_p^* / \eta L_m$, where the coefficient $\eta \equiv 1.414 R_c / L_m$ for cohesive soils and $\eta \equiv 1.5 R_c / L_m$ for cohesionless soils. From the idealized trilinear response, the plastic displacement, Δ_p^* , is related to the lateral strength and reduced stiffness of the soil-pile system as follows: $\Delta_p^* = (K_p / K_{rp})(V_u - V_y) / K_p$. Since $V_y = \alpha V_u$ and $V_u / K_p = \Delta_y = \beta \phi_y L_m^2$, Δ_p^* can be rewritten as $\Delta_p^* = (K_1 / K_2) \beta \phi_y L_m^2 (1 - \alpha)$. When the relation combined with $\mu_{\phi i}$, θ_p^* , and Δ_p^* , the curvature ductility, $\mu_{\phi i}$, can be determined:

$$\mu_{\phi i} = 1 + \frac{K_p}{K_{rp}} \frac{\beta L_m^*}{\eta \lambda_{p1}} (1 - \alpha) \quad (9)$$

where L_m^* is the normalized depth to the second plastic hinge and λ_{p1} is the normalized plastic hinge length of the first hinge. After determining the intermediate curvature ductility factor, $\mu_{\phi i}$, the ultimate determination of curvature ductility demand, $\mu_{\phi1}$, in the first plastic hinge can be defined utilizing Eq. (8) for a given displacement ductility factor, μ_Δ .

An estimation of the curvature ductility demand in the second plastic hinge is essentially required for the damage assessment of fixed-head piles, although the curvature ductility demand is possibly smaller than that of the first plastic hinge. In the

first plastic hinge, the rotation, θ_p^{**} , due to the plastic displacement of Δ_p^{**} is similarly written in terms of the ultimate curvature demand, ϕ_{u2} , and the equivalent plastic hinge length, L_{p2} , of the second hinge, i.e.: $\theta_p^{**} = (\phi_{u2} - \phi_y)L_{p2}$ for $\phi_{u2} \geq \phi_y$. Knowing the combination of θ_p^{**} for both soil conditions, it produces the plastic displacement, $\Delta_p^{**} = (\phi_{u2} - \phi_y)\lambda_{p2}L_m^*D^2$, where $\lambda_{p2} \equiv L_{p2} / D$ is the normalized plastic hinge length of the second hinge. Furthermore the same method for the first plastic hinge, the expressions for μ_Δ , Δ_y , μ_{ϕ_1} , and Δ_p^{**} may be written simultaneously to find the kinematic relation between the displacement ductility factor, μ_Δ , and the curvature ductility demand, μ_{ϕ_2} .

$$\mu_\Delta = \alpha + \frac{K_p}{K_{rp}}(1 - \alpha) + \frac{\lambda_{p2}}{\beta L_m^*}(\mu_{\phi_2} - 1) \quad (10)$$

The curvature ductility demand in the second plastic hinge is $\mu_{\phi_2} \equiv \phi_{u2} / \phi_y$. It should be noted that Eq. (10) is similar to the kinematic relation for the first plastic hinge in Eq. (8), except that the plastic hinge length is different and the curvature ductility demand at lateral displacement, Δ_{y2} , is equal to unity for the second plastic hinge.

The ultimate displacement imposed on the pile should be limited in a design displacement so that good performance of a pile-supported foundation may be achieved. When the design displacement sufficiently causes inelastic deformation in both plastic hinges, the curvature ductility demand is likely predicted using the kinematic relation between M_u^* and $p_u(x)$. In the case of a small lateral displacement ($\Delta_{y1} < \Delta_u < \Delta_{y2}$), only one plastic hinge will form at the pile head. To derive the kinematic relation for this condition, the displacement ductility factor, $\mu_\Delta = (\Delta_{y1} - \Delta_p') / \Delta_y$, is a function of the elastoplastic yield displacement, Δ_y , and the plastic displacement, $\Delta_p' \leq \Delta_p^*$. Similar to the θ_p^* , the plastic displacement, $\Delta_p' = \theta_p' \eta L_m$, is correlated to the plastic rotation of the first hinge, θ_p' , and the coefficient, η , for cohesive and cohesionless soils. Therefore the displacement ductility factor, μ_Δ is written as $\mu_\Delta = (\Delta_{y1} / \Delta_y) + (\eta L_{p1} L_m (\phi_{u1} - \phi_y) / \Delta_y$, where the plastic rotation $\theta_p' = (\phi_{u1} - \phi_y)L_{p1}$ and ϕ_{u1} is the ultimate curvature in the first plastic hinge. When $\alpha = \Delta_{y1} / \Delta_y$ and $\Delta_y = \beta \phi_y L_m^2$ are substituted into the μ_Δ equation, the relation between the displacement ductility factor, μ_Δ , and curvature ductility factor, μ_{ϕ_1} , for $\Delta_{y1} \leq \Delta_u \leq \Delta_{y2}$ is written as follows

$$\mu_\Delta = \alpha + \frac{\eta \lambda_{p1}}{\beta L_m^*}(\mu_{\phi_1} - 1) \quad (11)$$

where $\mu_{\phi_1} \equiv \phi_{u1} / \phi_y$. It is observed that the equivalent plastic hinge length for the first hinge of the fixed-head pile is adopted from that proposed by Priestly et al. (1996) as written in Eq. (12), where f_{ye} is the expected yield strength of the reinforcing steel and d_{bl} is the diameter of the longitudinal reinforcement of the pile.

$$L_{p1} = 0.04 L_m + 0.022 f_{ye} d_{bl} \geq 0.044 f_{ye} d_{bl} \quad (12)$$

where $\mu_{\phi 1} \equiv \phi_{u1} / \phi_y$ and f_{ye} is the expected yield strength of the reinforcing steel and d_{bl} is the diameter of the longitudinal reinforcement of the pile. The set of equations, namely Equations (8), (10) and (11), allows a full range of curvature ductility demand for fixed-head piles to be estimated. In a compact matrix form of Eq. (13), the displacement ductility factors, μ_{Δ} , for the first and second plastic hinges can be rewritten as follows:

$$\begin{Bmatrix} \mu_{\Delta 1} \\ \mu_{\Delta 2} \end{Bmatrix} = \begin{bmatrix} \left(\alpha - \frac{\eta \lambda_{p1}}{\beta L_m^*} \right) & \left(\frac{\eta \lambda_{p1}}{\beta L_m^*} \right) & 0 \\ \left(\alpha + \frac{K_p}{K_{rp}} (1 - \alpha) - \frac{\lambda_{p2}}{\beta L_m^*} \right) & 0 & \left(\frac{\lambda_{p2}}{\beta L_m^*} \right) \end{bmatrix} \begin{Bmatrix} 1 \\ \mu_{\phi 1} \\ \mu_{\phi 2} \end{Bmatrix} \quad (13)$$

4. RESULTS AND DISCUSSION

The curvature demand in the yielding region of a pile is related to the equivalent plastic hinge length of the pile. Studies of bridge columns or extended pile-shafts have resulted in empirical expressions for the equivalent plastic hinge length. In the case of fixed-head piles, it is reasonable to assume that the length of the first plastic hinge is similar to the plastic hinge length of a fixed-based bridge column, as the first plastic hinge of the pile forms against a supporting member. In this case, the equivalent plastic hinge length, L_{p1} , of the pile can be assumed to be the same as that of a fixed-based column, except that the height of the column is replaced by one-half of the distance to the second plastic hinge. This approach is based on the assumption that the bending moment in the upper region of fixed-head piles is similar to the reversed moment distribution in a laterally loaded column with full fixity at both ends. More specifically, the equivalent plastic hinge length for the first hinge of the fixed-head pile can be adopted from that proposed by Priestley et al. (1996). The equivalent plastic hinge length of the first plastic hinge, however, should not be taken as greater than the pile diameter. For the second plastic hinge, the spread of curvature will be more significant than that of the first plastic hinge. In this study, the equivalent plastic hinge length for the second plastic hinge is taken from the plastic hinge length for extended pile-shafts with a zero above-ground height (fully embedded in the soil strata), as proposed by Chai (2002), Chiou and Chen (2010). In this case, a plastic hinge length of $L_{p2} = D$, or a normalized plastic hinge length of $\lambda_{p2} = 1.0$, is appropriate for the second plastic hinge.

A proposed flow chart presented in Figure 4 is useful for the limit state analysis of a pile under lateral load for a fixed-head pile case in conjunction with the moment-curvature analysis. The first part of the flow chart includes material properties and geometric models. Having an input of reinforced concrete pile, a nonlinear cross-sectional analysis is performed to compute the moment-curvature. The moment-curvature response of the pile section is represented by an elastoplastic response resulting in an equivalent-elastoplastic yield curvature, ultimate bending moment, ultimate curvature, curvature ductility capacity and curvature ductility demand. Considering a reinforced concrete pile embedded in cohesive and cohesionless soils in the second part of the flow chart, this is then classified according to the NEHRP (2001) and is followed with different parameters to be computed. In the last part of the flow chart, using the same formulae, the relationship for displacement and curvature ductility demand can be computed.

A proposed routine of computer program incorporating the moment-curvature analysis was developed to analyze laterally loaded piles required matrix arrays for simplification program statements. It is noted that a routine of computer program integrating curvature ductility analysis into limit state analysis of laterally loaded pile was developed to take account for ductility demand of the fixed pile-to-pile cap connections embedded in two different soil conditions. For practical exercises, an application of simplified lateral load analyses of a fixed-head pile was briefly described in a companion paper (Teguh, 2009).

5. CONCLUSIONS

An analytical model for ductility assessment of the fixed pile-to-pile cap connections was summarized to determine kinematic relation between displacement and curvature ductility demands resulting a proposed flow chart. The conclusions are drawn based on the analytical development of the laterally loaded piles as follows.

- a. Analytical methods have been reviewed to simplify the integration of soil-pile interaction into the analysis and design of pile-to-pile cap connections. The limit state analysis incorporated the moment-curvature analysis to evaluate the capacity of a reinforced concrete pile.
- b. The proposed flow chart of the analysis has significantly helped to compute the lateral strength of the soil profile system, kinematic relation, and plastic hinge length. The flow chart demonstrates reliable results for a simple application of the pile-to-pile cap connection embedded in two different soil conditions, cohesive soil and cohesionless soil, under a laterally loaded pile.
- c. The effect of soil-structure interaction in design considerations reduces the base-shear applied to the structure, as well as the lateral forces and overturning moments, however it increases lateral displacements due to rocking. The use of a more refined soil-foundation interaction model for pile foundations will not necessarily lead to a more reliable prediction of foundation behavior, as the accuracy of the prediction will depend as much on the reliability of the soil data as upon refinement of the model.

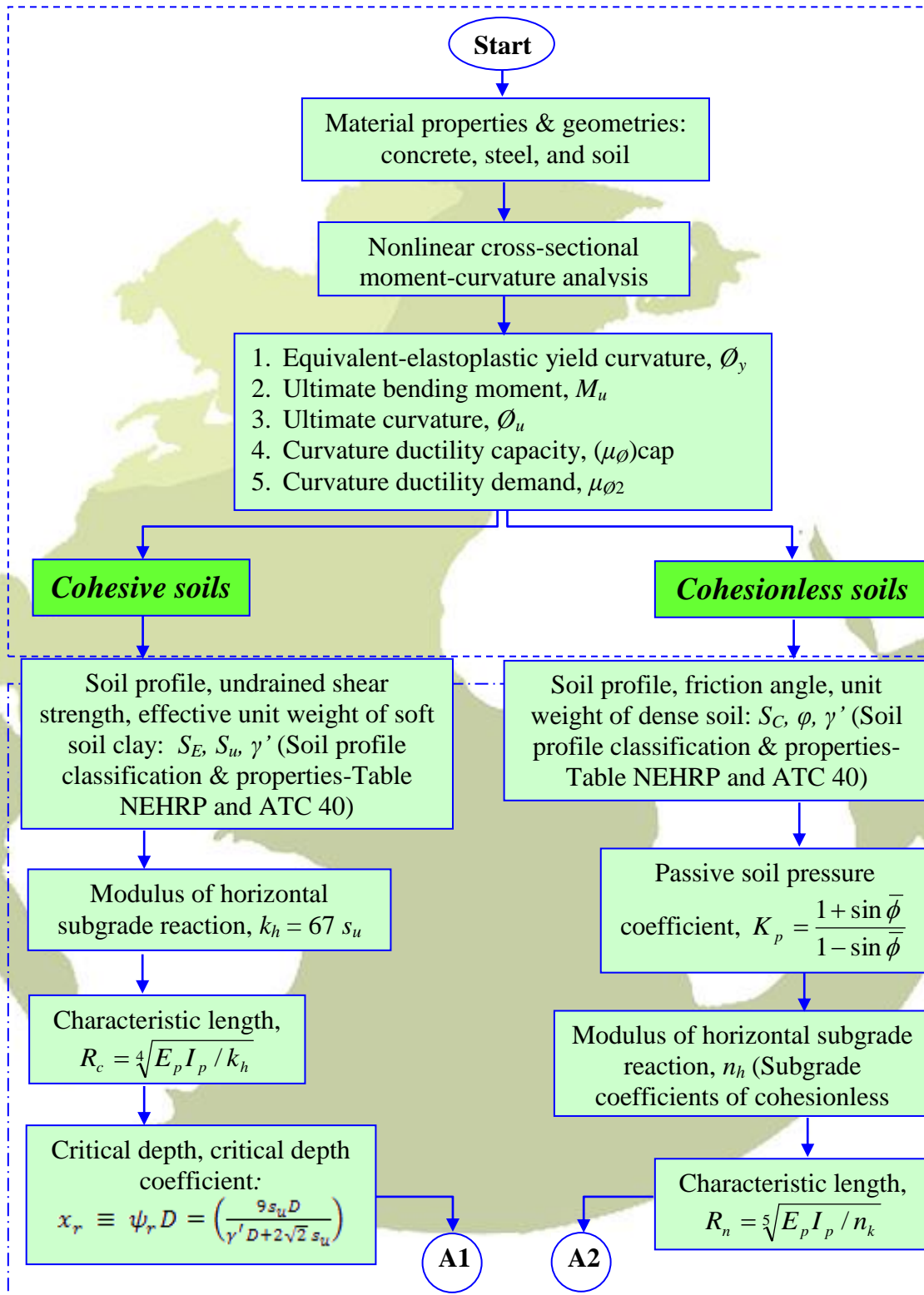


Figure 4. Flow chart of limit state analysis for a fixed-head laterally loaded pile

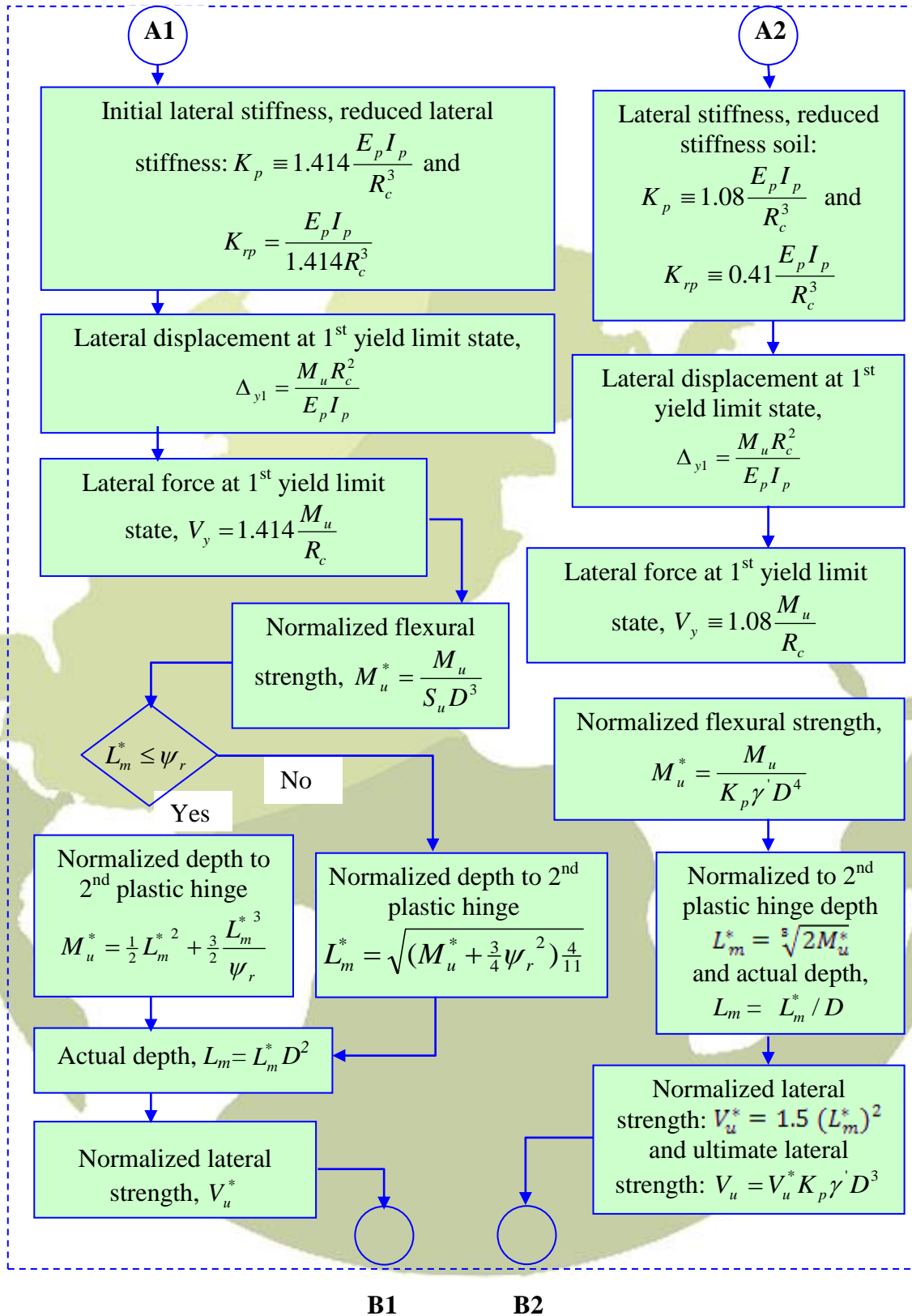


Figure 4. Flow chart of limit state analysis for a fixed-head laterally loaded pile (continued)

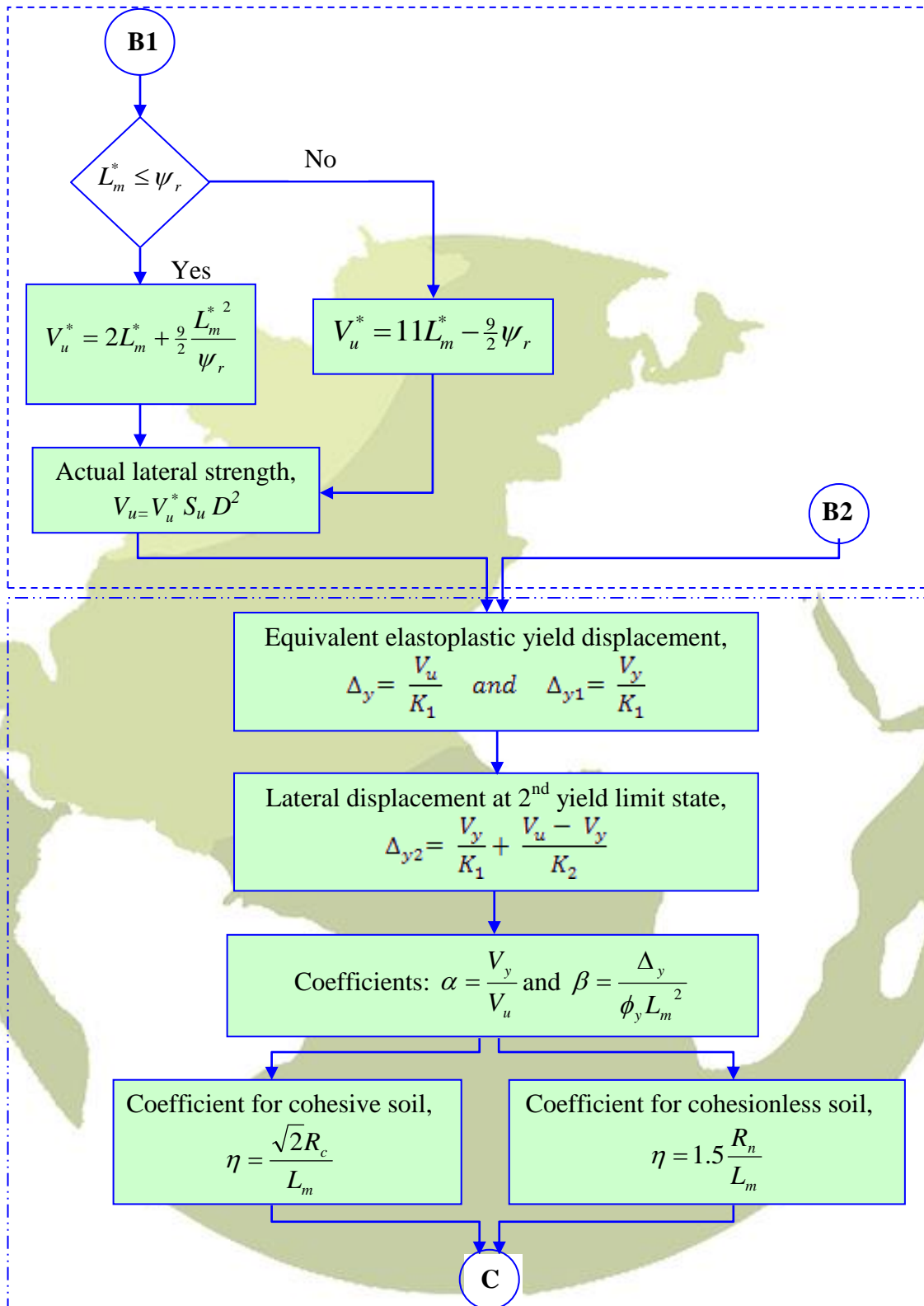


Figure 4. Flow chart of limit state analysis for a fixed-head laterally loaded pile (continued)

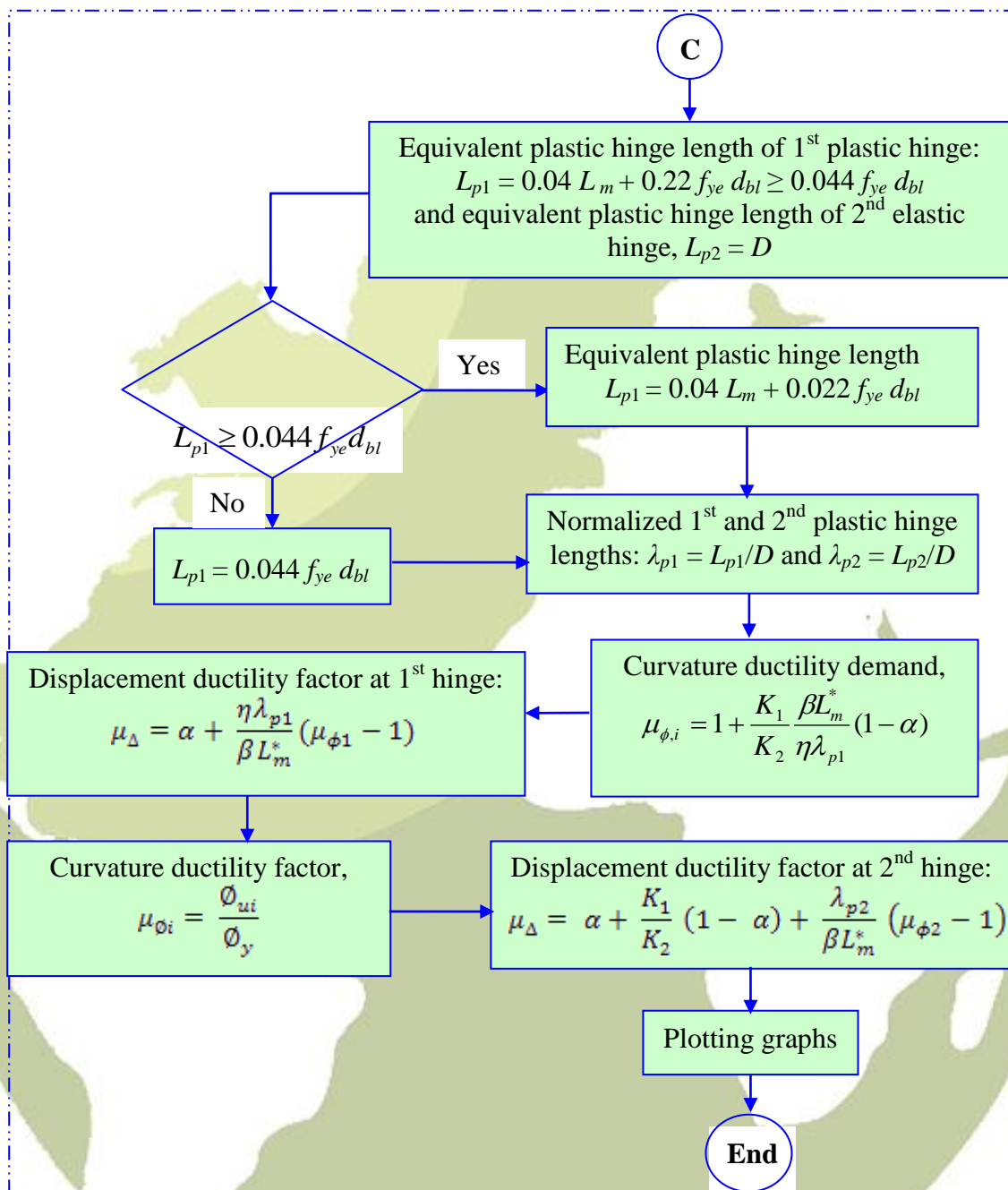


Figure 4. Flow chart of limit state analysis for a fixed-head laterally loaded pile (continued)

6. REFERENCES

ATC-32. (1996). *Improved Seismic Design Criteria for California Bridges: Provisional Recommendations*, Redwood City, California.
 ATC-40. (1996). *Seismic Evaluation and Retrofit of Concrete Buildings*, Redwood City, California.

- Broms, B. B. (1964). "Lateral Resistance of Piles in Cohesionless Soils." *Journal of Soil Mechanics and Foundation Division, ASCE*, 90(SM3), pp. 123-156.
- Chai, Y. H. (2002). "Flexural Strength and Ductility of Extended Pile-Shafts. I : Analytical Model." *Journal of Structural Engineering, ASCE*(May), pp. 586-594.
- Chiou, Jiunn-Shyang, and Chen, Cheng-Hsing (2010). Displacement Ductility Capacity of Fixed-Head Piles, Conference Proceeding of the Fifth International Conference on Recent Advances in Geotechnical Earthquake Engineering and Soil Dynamics, May 24-29, 2010, San Diego, California, USA, pp. 1-7.
- Davissou, M., and Salley, J. (1970). "Model Study of Laterally Loaded Piles." *Journal of Soil Mechanics and Foundation Division, ASCE*, Vol. 96, No. 5, 1605-1627.
- Gazetas, G., Fan, K., Tazoh, T., Shimizu, K., Kavvadas, M., and Makris, N. "Seismic Pile-Group-Structure Interaction." *Piles under Dynamic Loads*, New York, pp. 56-91.
- Holmes, W. T. (2000). "The 1997 NEHRP Recommended Provisions for Seismic Regulations for New Building and Other Structures." *Earthquake Spectra*, Vol. 16, No. 1, pp. 101-114.
- Matlock, H., and Reese, L. C. (1960). "Generalized Solutions for Laterally Loaded Piles." *Journal of Soil Mechanics and Foundation Division, ASCE*, 86(SM5), pp. 63-91.
- Meymand, P. J. (1998). "Shaking Table Scale Model Tests of Nonlinear Soil-Pile-Superstructure Interaction in Soft Clay," Ph.D thesis, University of California, Berkeley, California.
- NEHRP. (2001). *NEHRP Recommended Provisions for Seismic Regulations for New Buildings and Other Structures, FEMA 368*, Washington, D. C.
- Poulos, H. G., and Davis, E. H. (1980). *Pile Foundation Analysis and Design*, Wiley, New York.
- Priestley, M. J. N., Seible, F., and Calvi, G. M. (1996). *Seismic Design and Retrofit of Bridges*, Wiley, New York.
- Reese, L. C., and Van Impe, W. F. (2001). *Single Piles and Pile Groups under Lateral Loading*, Balkema, Rotterdam.
- Song, S. T., Chai, Y. H., and Hale, T. H. (2005). "Analytical Model for Ductility Assessment of Fixed-Head Concrete Piles." *Journal of Structural Engineering, ASCE*, Vol. 131, No. 7, pp. 1051-1059.
- Teguh, M. (2009). "Ductility Assessment of Reinforced Concrete Pile-to-Pile Cap Connections in Application", *Journal of Dinamika Teknik Sipil*, Vol. 9, No. 1, Januari 2009 (accredited by Dikti), Muhammadiyah University of Surakarta, pp. 1-8.
- Yang, Z. H., and Jeremic, B. (2002). "Numerical Analysis of Pile Behavior under Lateral Loads in Layered Elastic-plastic Soils." *International Journal for Numerical and Analytical Methods in Geomechanics*, Vol. 26 No. 14, pp 1385-1406.